

文章编号: 1006-9941 (2016)09-0892-06

Fabrication and Flyer Driving Capability Characterisation of an Integrated Exploding Foil Initiator

FANG Kuang, CHEN Qing-chou, FU Qiu-bo, WANG Yao

(Institute of Chemical Materials, China Academy of Engineering Physics, Mianyang 621999, China)

Abstract: An integrated exploding foil initiator (EFI) based on a parylene-C flyer and Su8 photo-resist barrel was fabricated using magnetron sputtering, photolithography, and chemical vapor deposition (CVD). The effect of structure parameters of exploding foil, flyer and barrel on the loading capability of flyer was investigated by photonic Doppler. Results show that under the conditions of initiation voltage 2.6 kV, capacitance 0.2 μF , and discharge duration 1.2 μs , through the test, finding that the change of part of materials for EFI caused by integrated fabricating dose not significantly influence the loading capability of flyer. The EFI's driving process of parylene-C and polyimide flyer with identical dimension are similar to each other. The flyer driving capability of integrated EFI was consistent with that of classic EFI with same structure parameters. The HNS-IV can successfully be detonated by the integrated EFI.

Key words: exploding foil initiators; photonic doppler velocimetry; flyer; magnetron sputtering

CLC number: TJ55

Document code: A

DOI: 10.11943/j.issn.1006-9941.2016.09.013

1 Introduction

Miniaturization and integration are the promising uptrends for the development of exploding foil initiator to satisfy the reliability, compaction, and energy-efficient requirement of the initiation system for the next generation weapons^[1]. With the prosperity of semiconductor industry, some classic micro-electronic techniques have been utilized for the fabrication of highly integrated exploding foil initiators (EFI).

John H. Henderson and Thomas A. Baginski^[2] have brought out two novel silicon substrate slapper detonators, which are fabricated by conventional microelectronic techniques, the EFI components are all manufactured in a cavity on the silicon substrate, while the bow-tie foil is obtained by the selective metal deposition or the ion diffusion. O'Brien D W, Druce R L, et al^[3], fabricated a integrated EFI by just the film deposition technique. And Amish Desai et al^[4], integrated the foil bridge, flyer, and barrel on the same substrate by deposition and photolithography technique. In addition, in 2007, the LLNL proposed a three year project to develop the rapid prototyping technique for the highly integrated chip slapper detonator. Solventless vapor deposition, femtosecond laser,

and photolithography technique have been applied to realize the rapid prototyping of integrated slapper detonator^[5].

The micro-electronic technique has brought in some new material for the fabrication of integrated EFI such as silicon, photoresist, polyimide film and so on. While there is barely any report about the impact on the EFI's output performance caused by this kind of evolution. In the present work, we proposed a novel integrated EFI which was fabricated by the classic microelectronic technique. For the flyer driving capability characterization, the photonic doppler velocimetry has been taken to investigate the impact caused by size of foil, flyer, barrel, and the material of components on the flyers' driving capability. The study in the present work has been compared to the result of other researchers for a profounder comprehension of the initiation mechanism of EFI.

2 Fabrication Process

Fig. 1 gives us the fabrication route of the integrated EFI. To start with, the copper foil was deposited on a ceramic temper by the magnetron sputtering. Then, with the help of photolithography and etching technique, we got the foil bridge. The sizes (width \times thickness) of metal foil bridges are 0.3 mm \times 3 μm , 0.3 mm \times 4 μm , respectively.

The parylene-C flyer was deposited on the foil bridge and ceramic substrate through the chemical vapor deposition (CVD) process which could be divided into 3 steps. The 1st step is the evaporation of the solid dimeric polymer target at 150 $^{\circ}\text{C}$, with a pressure of 130 Pa. Then it's the splitting de-

Received Date: 2016-05-19; **Revised Date:** 2016-07-05

Biography: FANG Kuang (1987-), male, Master, major in Mechanical Engineering. Research Interest: MEMS Technique of Pyrotechnic Device. e-mail: kuangf302@caep.cn

Corresponding Author: WANG Yao (1986-), female, Master, major in Pyrotechnic device. e-mail: wangyaoindi@caep.cn

composition process at 680 °C, 160 Pa, and at this step we would get the activated parylene monomer; Finally, the parylene monomer will polymerize on the substrate at 25 °C, 10 Pa immediately.

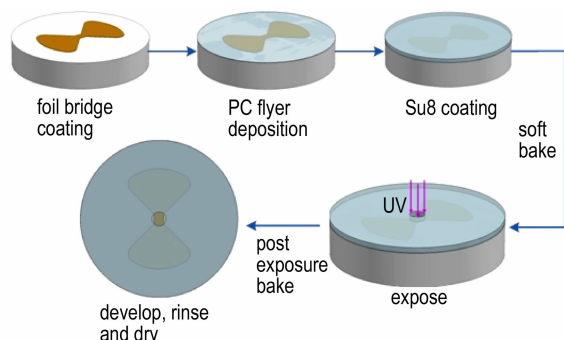


Fig. 1 Fabrication process of the integrated EFI

For the fabrication of barrel, the Su-8 photoresist was coated directly on the parylene-C film. After the development procedure, we would get the integrated EFI components. The detail of the integrated EFI components was illustrated in Fig. 2.

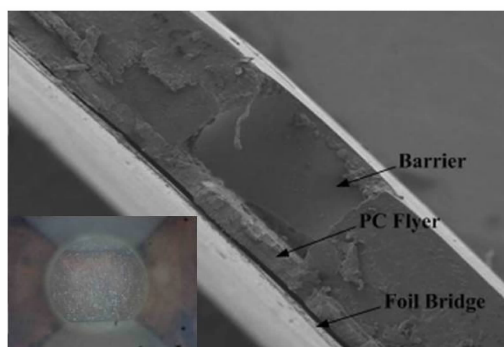


Fig. 2 SEM profile of EFI components

3 Experimental Techniques

An EFI system consists of a small capacitor charged by a high voltage, a switch, an exploding foil bridge, a plastic disk, a barrel and an explosive pellet. For velocity measurement, the explosive pellet is replaced by the laser probe of PDV, which could detect the mini flyer and measure the velocity of it. The scheme of the flyer launcher and probe configuration is illustrated in Fig. 3.

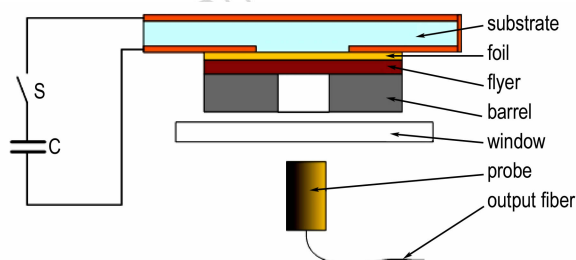


Fig. 3 EFI assembled with a flyer velocity diagnostic probe

The output fiber was connected to the experimental fixture, as shown in Fig. 4. The PDV probe positioned at about 6–10 mm away from the EFI assembly, in addition, there is a optic glass window between them for the protection of probe from impact damage.



Fig. 4 Picture of EFI assembly on experiment platform

After the firing set triggered, the foil bridge exploded immediately. Then the parylene-C film would be sheared to form a flyer and subsequently accelerated to a high speed. The reflection of laser beam by the high speed flyer is collected by the probe of PDV system and the raw data of beat frequency signal would be recorded by the oscilloscope. In addition the Sliding Fast Fourier Transform (SFFT) is performed to extract the time resolved beat frequency from the captured signal for the determination of the flyer velocity.

The PDV system was carried out by reflecting a single-mode laser beam from a moving surface, and then combining the reflected beam with a portion of the original beam, which would produce a beat frequency between the two signals, related to the velocity by:

$$v = \frac{\lambda_{\text{laser}}}{2} f_{\text{beat}} \tag{1}$$

The original concept of velocity measurement is showed in Fig. 5.

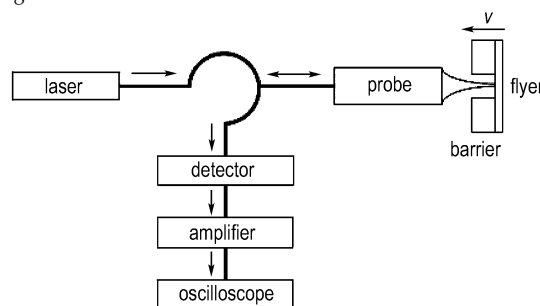


Fig. 5 The constitution of the PDV flyer velocity diagnostic system

4 Analyses and Discussion

4.1 Influences of Components Material on the Flyer Acceleration Capability of EFI

In the present work, the bridge width of all the test sam-

ples are identical 300 μm, and all the tests were conducted in the same firing set, the capacitance is 0.2 μF, the charging voltage 2.6 kV and the discharge duration 1.2 μs.

To investigate the influence of components material on the flyer acceleration capability, we've set 4 test groups, the parameters were listed in Table 1. The flyers' acceleration histories have been recorded by the PDV system.

Table 1 The sample parameters of EFI

sample	foil thickness / μm	barrel length / mm	barrel material	flyer thickness / μm	flyer material
1#	3	0.4	Su8	40	polyimide
2#	3	0.4	Su8	40	parlylene-C
3#	3	0.4	Steel	40	polyimide
4#	3	0.4	Steel	40	parlylene-C

Fig. 6 gives us the acceleration history comparison of different flyers, Fig. 6a Su8 barrel, Fig. 6b Steel barrel. As it shown in Fig. 6a, it seems that the flyer acceleration profiles matched with each other quite well, and for Fig. 6b the velocity discrepancy is no more than 5%. Though there is a density divergence between 1.35 g · cm⁻³ of parlylene-C flyer and 1.42 g · cm⁻³ of polyimide flyer, the divergence might be absorbed by the substrate binding force discrepancy between CVD method and normal assembly process.

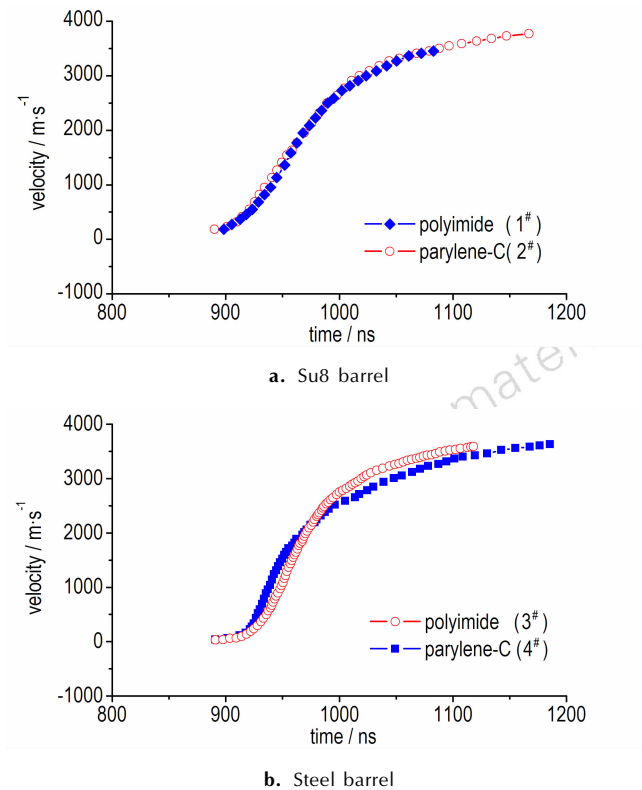


Fig. 6 Flyer velocity diagnostic of EFI assemblies with different flyer material

As it illustrated in Fig. 6, there isn't distinct disparity of flyer acceleration capability between parlylene-C and polyimide. Based on this premise, we set another firing test to check impact of the epoxy based photoresist barrel (Su8) on the flyer's acceleration. Fig. 7 gives us the flyer acceleration details between different barrels, Fig. 7a polyimide flyer, and Fig. 7b parlylene-C flyer.

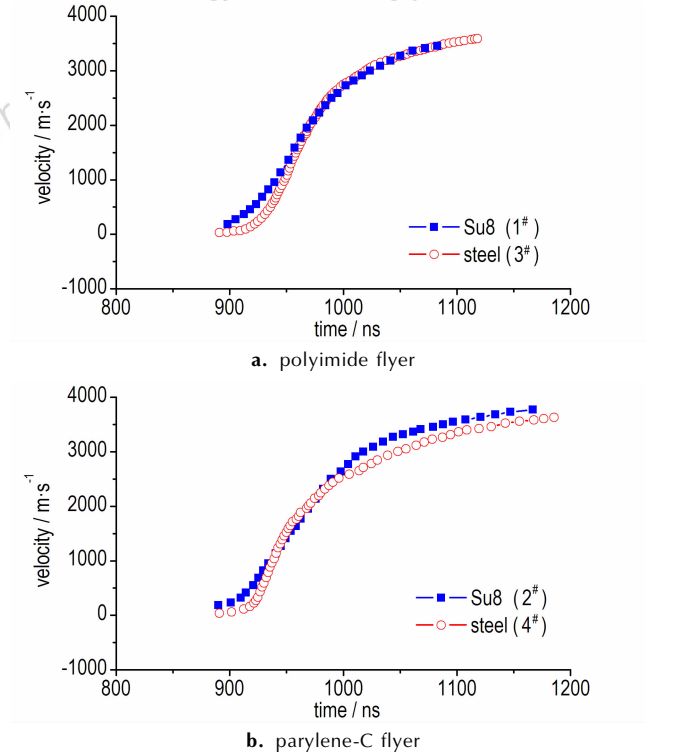


Fig. 7 Flyer velocity diagnostic of EFI assembled with different barrel material

As it shown in Fig. 7, the EFI with Su8 photoresist barrel (1#, 2#) provide us the similar flyer acceleration profile comparing with the EFI which is consist of steel barrel (3#, 4#). Though the flyer velocity at the impaction point 0.4 mm is different in Fig. 7b, 3454.5 m · s⁻¹ (2#) and 3312.9 m · s⁻¹ (4#), the disparity is within 4%. In addition, all the flyers have reached to 75% of the ultimate velocity in the first 80 ns, which is consistent with the test result of Chen^[6], and the VISAR diagnostic profile of Hatt^[7].

4.2 Influences of Foil Thickness on the Flyer Acceleration Capability

To investigate the impact of foil thickness on flyer acceleration capability of integrated EFI, we've set 2 test groups with different foil thickness, but identical flyer and barrel dimension. The parameters were listed in Table 2.

The acceleration profiles recorded by the PDV system were exhibited in Fig. 8, the flyer of sample 1# accelerated much faster than that of sample 2# at the beginning of accelera-

tion process, while it has been caught up by the flyer from sample 2[#] at the 100 ns from the start point. According to the same input energy, the thinner foil provides greater energy density while the thick foil would create more plasma for acceleration relatively. The greater energy density produces a faster electrical burst and better initial acceleration, while the larger quantity of plasma provides a more continuous acceleration. The combination of these factors could lead to the phenomena that exhibited in the Fig. 8.

Table 2 The sample parameters of EFI foil thickness test

sample	foil thickness / μm	barrel length /mm	barrel material	flyer thickness / μm	flyer material
1 [#]	3	0.4	Su8	25	parylene-C
2 [#]	4	0.4	Su8	25	parylene-C

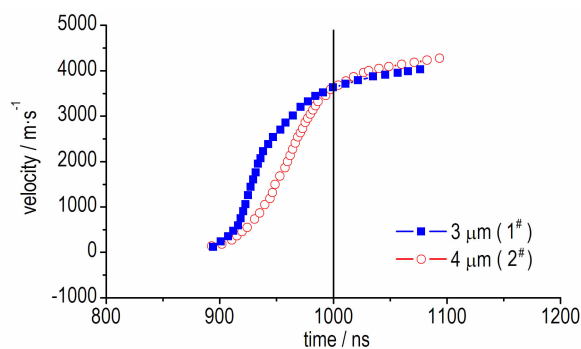


Fig. 8 The acceleration profile of flyers driven by exploding foil with different thickness

To investigate the velocity at impact point (the velocity at the barrel exit) during the flyers' flight, the flyer velocity-distance profile could be obtained from the integral of velocity-time history in Fig. 8.

As it illustrated in Fig. 9, The flyers' velocity at the impact point (0.4 mm) are respectively $3906 \text{ m} \cdot \text{s}^{-1}$ (1[#]) and $4129 \text{ m} \cdot \text{s}^{-1}$ (2[#]), the divergence of them is merely about 5%, which is consistent with the tests conducted by Jun-Sik Hwang, that the mean firing energy stays in a comparative level, when the foil thickness range from $3 \mu\text{m}$ to $6 \mu\text{m}$ ^[8].

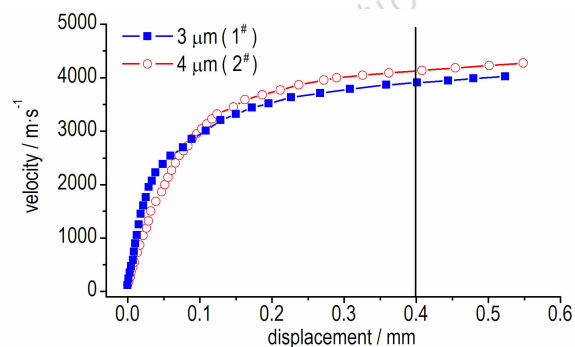


Fig. 9 The velocity-displacement profile of EFI assembled with different foil thickness

4.3 Influences of Barrel Length on the Flyer Acceleration Capability

The velocity at the impact point is one of the key factors for the initiation, and the impact point of flyer's flight is determined by the length of barrel. An unusual phenomenon was found that the mean threshold voltage of EFIs increases about 18% as the barrel length extends from 0.2 mm to 0.4 mm^[9]. For the investigation of flyers' acceleration process in these two kinds of barrel, we've set another test for the flyer velocity PDV diagnostic; the parameters are listed in Table 3.

Table 3 The sample parameters of EFI barrel length test

sample	foil thickness / μm	barrel length /mm	barrel material	flyer thickness / μm	flyer material
1 [#]	4	0.2	Su8	25	parylene-C
2 [#]	4	0.4	Su8	25	parylene-C

The result of the PDV diagnostic is illustrated in Fig. 10, which shows that there isn't any distinct divergence between the velocity profile of sample 1[#] and 2[#]. The flyer velocity at the flight distance of 0.2 mm could reach to 92% (1[#]) and 88% (2[#]) of the ultimate velocity detected, which is consistent with the velocity profile of Chow^[10]. The velocity at the impact point of 1[#](0.2 mm) and 2[#](0.4 mm) are respectively $3790 \text{ m} \cdot \text{s}^{-1}$ (1[#]) and $4129 \text{ m} \cdot \text{s}^{-1}$ (2[#]). With the barrel length extend from 0.2 mm to 0.4 mm; the velocity at impact point has increased about 9%.

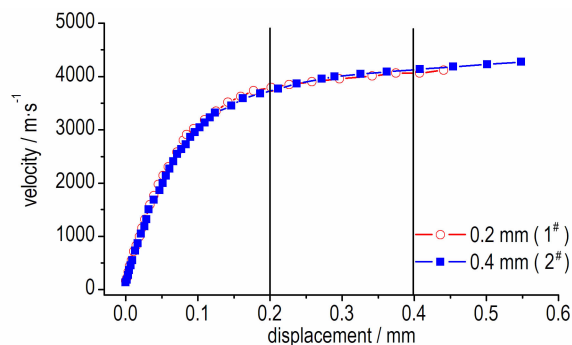


Fig. 10 The velocity-displacement profile of EFI assembled with different barrel length

As it shown in Fig. 10 that the velocity at the impact point indeed increased as the barrel length extended, which could deduced that the increasing of the mean threshold voltage should not own to the flyer velocity.

Actually, other factors may also associate with the flyer initiation energy, such as impact angle, impact area, and impact duration. After the vaporization of metal bridge, the flyer's driving pressure decreases sharply from the peak to a relatively low level. Under the influence of the driving pres-

sure transition, the flyer pose would get worse as barrel length extends. The flyer might incline as the flight distance extended, which would cause a larger contact angle and smaller interface of impact, and consequently enlarge the initiation energy because of diameter effect. In addition the ablation of hot plasma will increase synchronally as barrel length increase from 0.2 mm to 0.4 mm, which will leads to the cripple of flyer's impact duration, and meanwhile enlarge the initiation energy. Although the flyer velocity at 0.4 mm is higher than the one at 0.2 mm, the combination of the other adverse factors may lead to the increasing of mean threshold voltage^[9]. The influencing proportion of those ingredients needs more profound research.

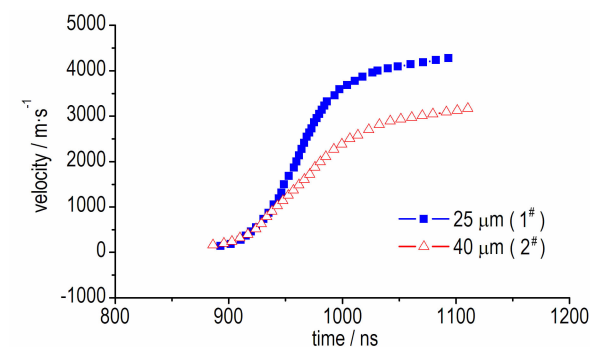
4.4 Influences of Flyer Thickness

The effect of flyer thickness on the flyer acceleration has also been investigated by the PDV diagnostic system. The test samples were set with different flyer thickness but the other parameters are identical as listed in Table 4.

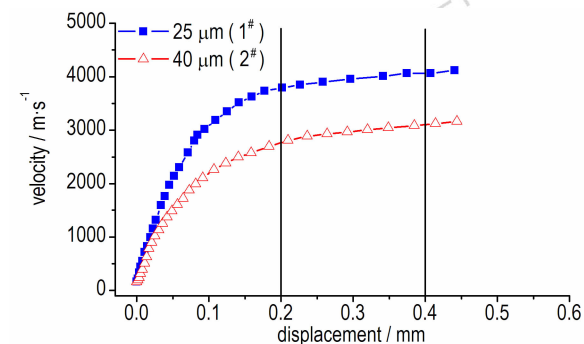
As it illustrated in Fig. 11a, the flyer of sample 1[#] accelerates much faster than that of 2[#], the maximum of flyer velocity

Table 4 The sample parameters of EFI flyer thickness test

sample	foil thickness / μm	barrel length /mm	barrel material	flyer thickness / μm	flyer material
1 [#]	4	0.4	Su8	25	parlylene-C
2 [#]	4	0.4	Su8	40	parlylene-C



a. time-velocity profile of flyer acceleration



b. time-displacement profile of flyer acceleration

Fig. 11 Flyer velocity diagnostic of EFI assembled with different flyer thickness

are respectively $4273 \text{ m} \cdot \text{s}^{-1}$ and $3164 \text{ m} \cdot \text{s}^{-1}$. In addition, as it exhibited in Fig. 11b, in the first 0.2 mm, the flyer velocity could reach to $3791 \text{ m} \cdot \text{s}^{-1}$ (1[#]), and $2793 \text{ m} \cdot \text{s}^{-1}$ (2[#]), the velocity of flyer $25 \mu\text{m}$ is 36% higher than that of flyer $40 \mu\text{m}$, while at the impact point 0.4 mm, the increment decrease to 30%.

The phenomena reveal that the thicker flyer lacks the ability of fast acceleration and thereby needs a longer barrel to obtain a higher velocity relatively. For the thin flyer, the velocity is able to reach the maximum in a short distance. While considering the ablation of hot plasma, a longer barrel doesn't necessarily guarantee better flyer acceleration.

4.5 The Firing Test of HNS-IV

For the detonation capability evaluation, the integrated EFI was assembled with the HNS-IV, as illustrated in Fig. 12. The firing condition was listed in Table 5. The dimension of the pellet is $\Phi 4 \text{ mm} \times 4 \text{ mm}$, the density is $1.58 \text{ g} \cdot \text{cm}^{-3}$. The function time was detected by the probe attached to the explosive.

Table 5 The firing condition for the detonation of HNS-IV

sample	voltage /V	barrel material	flyer material	function time / μs
1 [#]	2700	Su8	Parylene-C	1.00
2 [#]	2700	Su8	Parylene-C	1.06
3 [#]	2100	Su8	Parylene-C	-

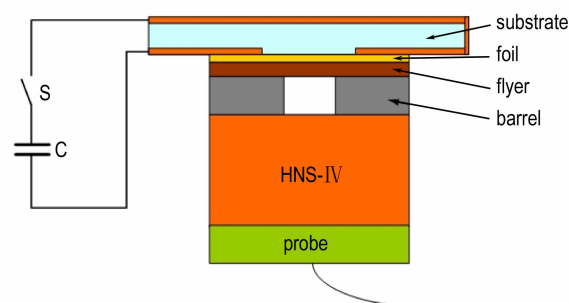


Fig. 12 Firing test of integrated EFI

As listed in table 5, the integrated EFI could successfully detonate the HNS-IV with a firing voltage above 2700 V, the function time is around $1.00 \mu\text{s}$, which is $0.1 \mu\text{s}$ higher than that of the conventional EFI with a polyimide flyer, the reason for this phenomenon, might due to substrate bonding force divergence caused by the different fabrication process of parylene-C and polyimide flyer, while the profounder explanation need further research.

5 Conclusions

In the present work, we proposed the fabrication process of an integrated EFI which was effective for the detonation of HNS-

IV. And for the flyer driving capability characterization, the PDV diagnostics have been applied to record the flyer acceleration history. The impacts of foil thickness, barrel length, flyer thickness, and components material have been investigated through the flyer acceleration profile. The results indicated that:

(1) For the investigation of flyer driving capability of the integrated EFI, there isn't distinct divergence of the overall flyer acceleration effect between the test sample with a foil thickness of 3 μm and 4 μm . While due to the greater energy density the sample with a foil thickness of 3 μm , indeed, provide better acceleration capability in the initial part of the flyer's flight.

(2) The longer barrel will provide more space for the flyer acceleration to reach a higher speed before the impact point; meanwhile it will also provide more opportunity for the cripple of the flyer's impact pose, which may lead to the increase of the mean threshold voltage.

(3) The thicker flyer lacks the ability of fast acceleration and thereby needs a longer barrel to obtain a higher velocity relatively. While for the thinner one, the velocity is able to reach the maximum in a shorter distance. Thus, considering the ablation of hot plasma, a longer barrel won't guarantee better flyer acceleration.

(4) The fabrication process of the integrated EFI in the present work is quite different from the classic one, but their overall flyer driving capabilities are similar to each other. Though there is a density divergence between 1.35 $\text{g} \cdot \text{cm}^{-3}$ of parylene-C flyer and 1.42 $\text{g} \cdot \text{cm}^{-3}$ of polyimide flyer, it might be absorbed by the substrate binding force discrepancy between CVD method and normal assembly process. In addition, comparing with steel barrel, the Su8 photoresist barrel could also fully competent for the flyer acceleration under the influence of foil's electrical exploding.

Acknowledgement: The support of this work by co-workers in Pyrotechnics Laboratory, Institute of Chemical Materials, CAEP is gratefully acknowledged.

References:

- [1] Prinse W, Scholtes G. A development platform for a microchip EFI[C]//The 52nd Annual Fuze Conference, Sparks, NV, May 13-15, 2008.
- [2] Henderson John H, Baginski Thomas A. Two novel monolithic silicon substrate slapper detonators[C]//Industry Applications Society Annual Meeting, 1993, 3: 2479-2482.
- [3] O'Brien D W, Druce R L, Johnson G W, et al. Method and system for making the integrated solid-state fire-sets and detonators: US,5731538[P].1998.
- [4] Amish Desai, Altadena, CA. Efficient exploding foil initiator and process for making same: US,7938065 B2[P].2011.
- [5] Mark A Schmidt. Chip Slapper Detonator Processing for Rapid Prototyping and Hydrodynamic Properties[R]. FY07 Engineering Research and Technology Report, Lawrence Livermore National Laboratory 2007: 100-101.
- [6] CHEN Qing-Chou, CHEN Lang, QIN Wen-Zhi et al. Photonic doppler velocimetry of mini flyers driven by electrically exploded foils[J]. *Journal of Energetic Material*, 2014, 22(3): 413-416.
- [7] David J Hatt. A VISAR Velocity Interferometer System at MRL for Slapper Detonator and Shockwave Studies[R]. Military Research Laboratory Report (Military Research Laboratory, Los Alamos, NM, USA, 1991), Report No. MRL-TR-91-42.
- [8] Jun-Sik Hwang, Moon-Ho Lee, Sang-Moo Lee, et al. A study on the factors affecting the fire sensitivity of exploding foil initiators[C]//31st International Pyrotechnics Conference, Fort Collins, Colorado, USA, June 11-16, 2004.
- [9] CHEN Qing-Chou, FU Qiu-Bo, CHEN Lang, et al. Parametric influences on the sensitivity of exploding foil initiators[J]. *Propellants, Explosives, Pyrotechnics*, 2014, 4(39): 558-562.
- [10] Chow R, Schmidt M, Advanced initiation systems manufacturing level 2 milestone completion summary[R]. Report LLNL-TR-417546, Lawrence Livermore National Laboratory, Livermore, CA, USA, 2009.

集成爆炸箔起爆器的制备和飞片驱动能力表征

房 旷, 陈清畴, 付秋菠, 王 窈

(中国工程物理研究院化工材料研究所, 四川 绵阳 621999)

摘要: 利用磁控溅射、光刻、化学气象沉积等技术制备了一种基于氯代对二甲苯(PC)飞片与 Su-8 光刻胶加速膛的集成爆炸箔起爆器(EFI), 利用光子多普勒技术研究了爆炸箔、飞片, 以及加速膛结构参数对飞片加载能力的影响作用。结果表明, 在起爆电压 2.6 kV, 电容 0.2 μF , 作用时间 1.2 μs 的条件下, 集成制造所引发的 EFI 部分材料的变化并未对其飞片加载能力带来显著影响, 相同尺寸的聚酰亚胺飞片与 PC 飞片的加速历程较为相近, 且集成 EFI 飞片加载能力与结构参数相同的常规 EFI 相当。利用该集成 EFI 能成功起爆 IV 型六硝基芪。

关键词: 爆炸箔起爆器; 光子多普勒测速; 飞片; 磁控溅射

中图分类号: TJ55

文献标志码: A

DOI: 10.11943/j.issn.1006-9941.2016.09.013